Molecular Cancer Research

# Discovery and Characterization of Recurrent, Targetable ALK Fusions in Leiomyosarcoma

Lara E. Davis[1,4], Kevin D. Nusser[1], Joanna Przybyl[2], Janét Pittsenbarger[1], Nicolle E. Hofmann[4], Sushama Varma[2], Sujay Vennam[2], Maria Debiec-Rychter[3], Matt van de Rijn[2], and Monika A. Davare[4]

## Abstract

Soft-tissue sarcomas such as leiomyosarcoma pose a clinical challenge because systemic treatment options show only modest therapeutic benefit. Discovery and validation of targetable vulnerabilities is essential. To discover putative kinase fusions, we analyzed existing transcriptomic data from leiomyosarcoma clinical samples. Potentially oncogenic ALK rearrangements were confirmed by application of multiple RNA-sequencing fusion detection algorithms and FISH. We functionally validated the oncogenic potential and targetability of discovered kinase fusions through biochemical, cell-based (Ba/F3, NIH3T3, and murine smooth muscle cell) and *in vivo* tumor modeling approaches. We identified ALK rearrangements in 9 of 377 (2.4%) patients with leiomyosarcoma, including a novel KANK2-ALK fusion and a recurrent ACTG2-ALK fusion. Functional characterization of the novel ALK fusion, KANK2-ALK, demonstrates it is a dominant oncogene in Ba/F3 or NIH3T3 model systems, and has tumorigenic potential when introduced into smooth muscle cells. Oral monotherapy with targeted ALK kinase inhibitor lorlatinib significantly inhibits tumor growth and prolongs survival in a murine model of KANK2-ALK leiomyosarcoma. These results provide the first functional validation of a targetable oncogenic kinase fusion as a driver in a subset of leiomyosarcomas. Overall, these findings suggest that some soft-tissue sarcomas may harbor previously unknown kinase gene translocations, and their discovery may propel new therapeutic strategies in this treatment-refractory cancer.

**Implications:** A subset of leiomyosarcomas harbor previously unrecognized oncogenic ALK fusions that are highly responsive to ALK inhibitors and thus these data emphasize the importance of detailed genomic investigations of leiomyosarcoma tumors.

## Introduction

Soft-tissue sarcomas (STS) are a heterogeneous group of rare tumors of mesenchymal origin. Despite multimodal treatment including surgery, chemotherapy, and radiation, STS frequently portend a poor prognosis (1–3). Discovery and validation of oncogenic drivers and cognate-targeted therapies has the potential to dramatically impact patient outcomes by providing more effective, less morbid treatment.

Constitutively activated kinase fusions arising from somatic chromosomal rearrangements are known drivers of malignant transformation (4). Approximately 20% of sarcomas have well-known translocations, such as the *SS18-SSX* fusion in synovial sarcoma. However, few rearrangements found in sarcomas involve a kinase partner, and thus are not targetable with currently available small-molecule inhibitors. The exceptions are in rare, locally aggressive tumors, including dermatofibrosarcoma protuberans (*COL1A1-PDGFB*) and tenosynovial giant cell tumors (*COL6A3-CSF1*) and infantile fibrosarcoma (*ETV6-NTRK3*; refs. 5–7). Targetable nonfusion kinase alterations have been identified in a handful of sarcoma subtypes, most notably activation of cKIT and PDGFR receptors in gastrointestinal stromal tumors (GIST), where treatment with kinase inhibitors has dramatically changed prognosis (8).

Leiomyosarcoma is the second most common sarcoma, with approximately 2,000 newly diagnosed patients per year (9–11). Leiomyosarcomas originate from smooth muscle, most often of the uterus, retroperitoneum, or blood vessels, and leiomyosarcomas frequently develop resistance to standard cytotoxic chemotherapy (12). The genomic landscape of leiomyosarcoma tends to be complex, and previously there was no indication of actionable or recurrent gene rearrangements. The Cancer Genome Atlas (TCGA) Research Network's comprehensive characterization of soft-tissue sarcomas included 80 leiomyosarcoma specimens; no oncogenic kinase fusions were reported (13). However, multiple targetable kinase fusions were reported previously from a set of 967 sarcomas sequenced by Foundation Medicine as a part of clinical care (14, 15). In that study, we identified 5 leiomyosarcomas with ALK fusions, leading us to hypothesize that ALK fusions may be an underappreciated and therapeutically targetable occurrence within a clinically meaningful subset of patients with leiomyosarcoma.

[1]Knight Cancer Institute, Oregon Health and Sciences University, Portland, Oregon. [2]Department of Pathology; Stanford University School of Medicine, Stanford, California. [3]Department of Human Genetics, KU Leuven and University Hospitals Leuven, Leuven, Belgium. [4]Division of Pediatric Hematology/Oncology, Department of Pediatrics, Oregon Health and Sciences University, Portland, Oregon.

**Note:** Supplementary data for this article are available at Molecular Cancer Research Online (http://mcr.aacrjournals.org/).

Corrected online August 15, 2019.

**Corresponding Authors:** Monika A. Davare, Oregon Health & Science University, 3181 SW Sam Jackson Park Road, Mail Code L587, Portland, OR 97239. Phone: 503-494-5056; Fax: 503-418-5044; E-mail: davarem@ohsu.edu; Lara Davis, davisla@ohsu.edu

**doi:** 10.1158/1541-7786.MCR-18-1075

Anaplastic lymphoma kinase (*ALK*), a receptor tyrosine kinase, is primarily expressed in the developing central nervous system (CNS) and has weak to no expression in normal adult human tissues (16). Chromosomal rearrangements of the *ALK* gene generate chimeric ALK fusion proteins wherein the rearrangement retains the *ALK* kinase domain sequence with various in-frame 5′ partners (4). ALK rearrangements are established oncogenic drivers in a subset of non–small cell lung cancer (NSCLC; ref. 17), but have also been reported in several other malignancies, including in leukemia, B-cell lymphoma, inflammatory myofibroblastic tumor (IMT), and anaplastic large cell lymphoma (ALCL; refs. 4, 18–23).

The discovery of *EML4-ALK* in a subset of patients with NSCLC propelled the development of small-molecule ALK inhibitors. Crizotinib, the first FDA-approved ALK inhibitor, was rapidly implemented as standard of care for patients with ALK fusion–positive lung adenocarcinoma (24–28). Several second- and third-generation ALK inhibitors are now in clinical trials, including lorlatinib and entrectinib (29, 30), and three additional ALK inhibitors were recently FDA approved: ceritinib (Novartis, April 2014), alectinib (Hoffman-La Roche, December 2015), and brigatinib (Ariad, April 2017). ALK tyrosine kinase inhibitors are expected to offer significant therapeutic benefit to patients with ALK-rearranged malignancies beyond lung cancer.

Following the identification of 5 of 223 leiomyosarcomas with ALK fusions in the Foundation Medicine dataset (14), we explored the incidence, diversity and functional impact of ALK fusions in leiomyosarcoma in two additional independent cohorts, namely TCGA and a tissue microarray (TMA). We report the discovery and characterization of recurrent, targetable ALK rearrangements identified in these cohorts. We go on to demonstrate efficacy of clinically viable ALK tyrosine kinase inhibitors in multiple cell-based model systems and highlight that these fusions are oncogenic drivers in a lineage-specific murine model of leiomyosarcoma. Taken together, these data have immediate translational relevance to potentially impact diagnostic approaches, treatment, and prognosis in this aggressive cancer subtype.

## Materials and Methods

### Fusion identification

The TCGA RNA-seq data were downloaded from the dbGaP website, under phs000178.v8.p7 (31). We applied four different software packages for the identification of ALK rearrangements in RNA-Seq data of selected leiomyosarcoma TCGA cases: STAR-Fusion version 0.1.1 (32), ChimeraScan version 0.4.5 (33), deFuse version 0.6.2 (34), and FusionCatcher (35) version 0.99.5a. The fusion calling algorithms were run on the RNA-Seq fastq files with paired-end reads generated by Illumina HiSeq2000 instrument with the default settings.

### FISH

We employed a previously described TMA, TA-381, which includes 126 unique leiomyosarcoma donor samples (36). The FISH assay was performed to examine ALK rearrangement (Biocare Medical catalog no. 902-7000-082115) using 4-μm formalin-fixed paraffin-embedded (FFPE) sections. As per the manufacturer, the 3′ ALK probe was labeled in red (Ex 593 nm; Em 618 nm) while the 5′ ALK probe was labeled in green (Ex 498 nm; Em 522 nm). Slides were deparaffinized in xylene ×3 for 10 minutes, dehydrated twice with 100% ethanol, air dried for 10 minutes, and then pretreated in 10 mmol/L citric acid pH 6.0 at 80°C for 45 minutes. Samples on slides were digested for 60 minutes in pepsin (at 75,000 U, Sigma catalog no. P6887) at 37°C. Fluorescence-labeled probes and slides were codenatured at 75°C for 7 minutes and hybridized at 37°C for 16–18 hours in a humidified chamber. Posthybridization washes were performed using 2 × SSC/0.3% NP-40 at 72°C for 5 minutes. Slides were dehydrated and air-dried in the dark and counterstained with DAPI (catalog no. P36935 Invitrogen/Life Technologies), and followed by imaging. Probe deemed evaluable in 97 cases. Signals were scored by a cytogeneticist (M. Debiec-Rychter) by evaluating at least 50 tumor cell nuclei per case. A split signal was defined by 5′ and 3′ signals being observed at a distance greater than a single signal width, and signals separated by less than this were regarded as fused signals. Tumor cells showing split signals or isolated 3′ (red labeled) signals were considered to have rearrangements of ALK. We interpreted a result as FISH-positive if >20% of tumor cells showed gene rearrangement.

### PCR from FFPE tissue samples

Small sections of FFPE tumor tissue were excised, placed in xylene, and vortexed vigorously. Tissue homogenate was fractionated by centrifugation; the supernatant was discarded and the pellet was washed in ethanol by vortexing and recentrifugation, followed by air-drying of the ethanol-treated pellet. An RNA extraction kit (RNAeasy FFPE kit, Qiagen) was used to purify RNA from tissue and amount of RNA was quantified by measuring absorbance using the NanoDrop spectrophotometer. cDNA was made using VILO kit (Thermo Fisher Scientific). Primers used for amplification of ALK using PCR were TGATGATCAGGGCTTCCATG and CATCACCCTCATTCGGGGT taken from 20th exon. Primers for GAPDH were AGGGCTGCTTTTAACTCTGGT and CCCCACTTGATTTTG-GAGGGA. RT-PCR using VILO reagents were conducted on C1000 Touch Thermal Cycler (Bio-Rad) with a cycle of 94°C for 15 seconds, followed by 45 cycles of 94°C for 15 seconds, 56°C for 30 seconds, and 68°C for 30 seconds. PCR products were resolved on a 2% agarose gel and imaged using Gel DOC$^{tm}$ XR+ (Bio-Rad).

### Molecular cloning

ACTG2-ALK and KANK2-ALK cDNA were generated using GenScript gene synthesis service in pUC57 vector, and subsequently subcloned into the pMSCV-IRES-GFP retroviral vector using In-Fusion HD cloning (Clontech) following manufacturer's protocol. pMX-p53DD was a gift from Dr. Shinya Yamanaka, Kyoto University, Japan (Addgene plasmid # 22729; ref. 37), and the p53DD insert from this vector was subcloned into a pMSCV-IRES-mRFP retroviral vector using In-Fusion HD Cloning Kit (Clontech) to enable enrichment of dual GFP (ALK fusion) and mRFP (p53DD)-positive cells populations.

### Cell culture and retroviral transduction

Where indicated, retroviral particles were produced by transient transfection of the ecotropic viral packaging cell line, Platinum-E (Cell Biolabs) following manufacturer's protocol. Culture supernatant containing retroviral particles was collected 48 hours after transfection, and immediately used for transduction of recipient cells (Ba/F3, NIH3T3, or mSMCs).

Ba/F3 cells (ATCC) were cultured in RPMI1640 medium (Thermo Fisher Scientific) with 10% (vol/vol) FBS, L-glutamine, penicillin/streptomycin, and 15% (vol/vol) conditioned media produced from the WEHI-3 myelomonocytic IL3-secreting cells.

Ba/F3 cell lines were maintained at densities of 0.5 to 1.5 × $10^6$/mL and infected with retrovirus-encoding human KANK2-ALK and ACTG2-ALK fusion genes. Stable cell lines were generated after FACS for GFP. Cell number and viability were counted every 2–3 days. NIH 3T3 cells (ATCC) were cultured in DMEM-high glucose medium (Thermo Fisher Scientific) supplemented with 10% FCS, L-glutamine, and penicillin/streptomycin. Early-passage NIH 3T3 cells were transduced with KANK2-ALK and sorted for GFP expression as described for Ba/F3 cells. Primary uterine mouse smooth muscle cells (mSMC) from C57BL/6 mice were purchased from Cell Biologics, and cultured in growth media until 75% confluent. Normal mSMCs went into quiescence after 2 weeks, but colonies of transduced dnp53 mSMCs as detected by mRFP expression were clonally expanded; dnp53 expression induced mSMC immortalization without change to morphology. Once established, the mSMC dnp53 (p53DD) cell line was cultured in DMEM-high glucose medium supplemented with 10% FCS, L-glutamine, and penicillin/streptomycin. For bioluminescent imaging, stable mSMC dnp53 cells were transduced with firefly luciferase lentiviral particles (Cellomics Technology) and selected with blasticidin. In a final step, the mSMC dnp53 plus firefly luciferase cells were transduced with KANK2-ALK retroviral particles as described above.

### Inhibitor studies

For dose–response cell viability assays, Ba/F3 cell lines (1 × $10^3$ cells) were distributed in 384-well plates that had escalating concentrations of inhibitors (crizotinib, ceritinib, alectinib, lorlatinib, entrectinib, brigatinib) ranging from 1 pmol/L to 1 μmol/L, and incubated for 72 hours. Cell viability was measured using a methanethiosulfonate (MTS)-based assay (CellTiter96 Aqueous One Solution; Promega) and absorbance (490 nm) was read after 1 hour using the BioTek Synergy 2 plate reader. To facilitate comparison between experiments, the raw MTS absorbance of vehicle (0.1% DMSO)-treated cells was set to 1, and absorbance from inhibitor-treated wells was normalized to the vehicle-treated value. Each experiment had a minimum of three replicate wells per condition and the average and SEM was plotted for curve fit analysis. Assay was repeated on two additional days; results are from one representative experiment. Data were normalized using Microsoft Excel and further nonlinear regression curve fit analysis of the normalized data for determination of $IC_{50}$ values was performed using GraphPad Prism software.

### Immunoblotting

NIH3T3 or mSMC cells stably expressing KANK2-ALK were treated for 3 hours with vehicle, lorlatinib, crizotinib, and entrectinib at doses as indicated in Fig. 2. Immediately after treatment, the cells were washed once in Dulbecco PBS and collected in 100 μL of cell lysis buffer [20 mmol/L Tris-HCl (pH 7.5), 150 mmol/L NaCl, 1 mmol/L EDTA, 1 mmol/L EGTA, 1% Triton, 2.5 mmol/L sodium pyrophosphate, 1 mmol/L beta-glycerophosphate, 1 mmol/L sodium orthovanadate, 1 μg/mL leupeptin and 1 mmol/L phenylmethylsulfonyl fluoride]. Protein content was assessed by bicinchoninic acid assay (Thermo Fisher Scientific), and 40 μg of protein lysate was evaluated by gel electrophoresis and immunoblotting with following antibodies: total ALK (3633S, Cell Signaling Technology), phospho-ALK (3983S, Cell Signaling Technology), phospho-ERK1/2 (9101, Cell Signaling Technology), and GAPDH (AM4300, Thermo Fisher Scientific).

### *In vivo* tumorigenicity

All animal protocols were executed in compliance with institutional guidelines and regulations, and after approval from the OHSU Institutional Animal Care and Use Committee (protocol IP00000031). Eight-week-old female nude mice (The Jackson Laboratory) were injected with dnp53 mSMC or KANK2-ALK mSMC (1 × $10^6$ cells in 50 μL PBS) subcutaneously. *In vivo* luciferase imaging was performed 10 minutes after mice were injected (intraperitoneal) with luciferin (150 mg/kg, 15 mg/mL in sterile PBS, XenoLight D-Luciferin, PerkinElmer), using the IVIS system (IVIS Spectrum, Caliper Life Sciences). Mice were monitored for tumor engraftment, and once palpable, tumor growth was monitored using digital calipers (Fisher Scientific). Once tumor size reached 0.2 $cc^3$, mice were randomly assigned to one of the following treatment groups: vehicle alone ($n$ = 7, 0.5% methyl cellulose/0.5% Tween-80), lorlatinib ($n$ = 6, 3 mg/kg, provided by Pfizer via MTA and then prepared in 10% ethanol, 40% PEG200), or crizotinib ($n$ = 6, 100 mg/kg in 0.5% methyl cellulose/0.5% Tween-80; purchased from LC Labs). Each group was dosed via oral gavage once daily 5 days per week for 4 weeks. Mice were weighed and tumor measured thrice weekly. Once tumors reached 2 $cc^3$, animals were euthanized and tumors were harvested for biochemical (flash frozen) and IHC (10% zinc formalin) analyses. For on-target evaluation of lorlatinib on intratumoral ALK, small pieces of flash frozen, treated tumors were placed in liquid nitrogen and pulverized using a mortar and pestle prior to protein extraction with cell lysis buffer. Forty micrograms of tumor lysate was evaluated by immunoblotting as described above.

### Statistical analysis

Where indicated, the Student $t$ test (Microsoft Excel or GraphPad Prism) was used to determine statistical significance and comparisons; $P$ values less than 0.05 were deemed significant. Asterisks in figures and the description of asterisks in figure legends indicate level of statistical significance.

## Results

### ALK fusions are present in clinical leiomyosarcoma specimens

Kinase fusions are being reported at a low incidence across a wide variety of malignancies, leading to profound benefit for those patients (4, 6, 29, 38). Given the clear clinical need for improved therapeutic options, we sought to identify clinically relevant genomic alterations in sarcomas. We previously interrogated next-generation sequencing data performed as part of clinical care (14), and discovered *ALK* rearrangements in 5 of 223 leiomyosarcomas (Table 1, "FM-LMS" samples). The gene partner for FM-LMS5 was not identified; the Foundation Medicine raw sequencing data are proprietary but the Foundation Medicine analysis algorithms considered this fusion clinically reportable. Concurrent loss of *CDKN2A/B* and/or alteration of *TP53* was present in all five samples.

The frequency of *ALK* rearrangements specifically in leiomyosarcomas in the Foundation Medicine cohort prompted us to interrogate The Cancer Genome Atlas (TCGA) Network's sarcoma genomic dataset for evidence of *ALK* fusions. On the basis of the bioinformatics algorithm developed by Shah and colleagues (39), we assessed the publicly available TCGA sarcoma DNA copy number data (provisional dataset, available

**Table 1.** Leiomyosarcomas with evidence of ALK fusions from three independent cohorts. "FM-LMS" identified from Foundation Medicine and were reported previously (14, 15), from a total of 223 leiomyosarcoma sequenced. "TCGA" identified from The Cancer Genome Atlas (13), from a total 57 leiomyosarcoma evaluable by DNA copy number. "TA-381" identified from tumor microarray (36), from a total of 97 leiomyosarcoma evaluable by FISH. Unk, unknown

| Sample | Age | Gender | Uterine | 5′ Partner | Additional reports of same 5′ partner |
|---|---|---|---|---|---|
| FM-LMS-1 | 53 | F | Yes | *STK32B* | Ref. 14, 15 |
| FM-LMS-2 | 60 | F | Unk | *IGFBP5* | Ref. 14, 23 |
| FM-LMS-3 | 57 | F | Yes | *ACTG2* | Ref. 14, 15 |
| FM-LMS-4 | 49 | F | Unk | *TNS1* | Ref. 14 |
| FM-LMS-5 | 75 | M | No | Unk | |
| TCGA-IW-A3M6 | 59 | F | Yes | *ACTG2* | Ref. 14, 15 |
| TCGA-FX-A48G | 56 | F | Yes | *KANK2* | |
| TA-381-6806 | 56 | F | Yes | Unk | |
| TA-381-6871 | 59 | M | No | Unk | |

through cBioPortal; ref. 40) for 5′/3′ imbalances in the *ALK* gene. Three of 57 LMS samples demonstrated DNA copy number alterations within the *ALK* gene, suggestive of an unbalanced *ALK* rearrangement. Visualization of these data using the Integrative Genomics Viewer (41) indicated loss of a chromosomal segment just upstream of the *ALK* kinase domain. All three specimens were FNCLCC grade 2 uterine leiomyosarcoma (13).

Subsequent detailed analysis of raw RNA-sequencing data for two samples, TCGA-FX-A48G and TCGA-IW-A3M6, revealed novel fusion transcripts (Table 1; Fig. 1A and B; Supplementary Fig. S1). One of the three specimens showing genomic imbalance in the *ALK* gene (TCGA-IS-A3K7) did not have adequate read depth by RNA-Seq to validate the rearrangement. The *ACTG2-ALK* fusion found in TCGA-IW-A3M6 and the *KANK2-ALK* fusion identified in TCGA-FX-A48G are transcripts with unknown oncogenic potential, and *KANK2-ALK* has not previously been reported. The *ACTG2-ALK* fusion found in TCGA-IW-A3M6 was identified by DeFuse, FusionCatcher, and ChimeraScan, and the *KANK2-ALK* fusion in TCGA-FX-A48G was identified by DeFuse and ChimeraScan (Supplementary Table S1; Supplementary Figs. S2 and S3). Notably, the *ACTG2-ALK* discovered in the TCGA dataset was also independently identified in a distinct clinical sequencing sample, FM-LMS-3, from a separate cohort (Table 1). *ACTG2* (2p13.1) and *ALK* (2p23.2-p23.1) are located on chromosome 2p in opposite orientations, suggesting that a cryptic paracentric inversion is responsible for this rearrangement.

To validate ALK fusions in leiomyosarcoma and ascertain incidence, we examined ALK rearrangements in an independent leiomyosarcoma patient cohort. We assessed a leiomyosarcoma tissue microarray (TA-381) using FISH; all samples in the TMA underwent expert pathologic review prior to construction (36). Among 97 leiomyosarcoma cases evaluable by FISH, two samples exhibited *ALK* rearrangement as detected by ALK break-apart FISH probes (TA-381-6806 and TA-381-6871, Fig. 1C). Both of the ALK-rearranged cases expressed the ALK kinase domain as detected by reverse-transcriptase PCR (RT-PCR; Fig. 1D) while samples with normal FISH signal expressed detectable levels of ALK (representative example 6021 in Fig. 1D). We were unable to characterize the specific 5′ ALK fusion partner in the ALK-rearranged TMA samples, TA-381-6806 and TA-381-6871, due to insufficient tissue availability.

Because KANK2-ALK was previously uncharacterized, we assessed oncogenic potential. Three independent model systems were employed to test whether: (i) *KANK2-ALK* functions as a dominant, transforming oncogene in the well-established Ba/F3 model system; (ii) clinically-relevant ALK inhibitors effectively inhibit ALK catalytic activity and downstream signaling in KANK2-ALK expressing NIH3T3 murine fibroblasts; and (iii) *KANK2-ALK* drives tumor growth in an *in vivo*, lineage-specific murine tumor model.

### KANK2-ALK is a transforming oncogenic driver in Ba/F3 cells

Ba/F3, a pro-B murine cell line, is an established model system for investigating transformative potential of oncogenic kinase variants (42). Expression of constitutively activated tyrosine kinases, including kinase fusion oncogenes, confers IL3 independence to permit limitless replicative growth, thus transforming Ba/F3 cells. Stable expression of KANK2-ALK provided sufficient signaling drive for rapid and sustained IL3-independent Ba/F3 outgrowth, while cells expressing empty vector (pMSCV-PIG) were unable to grow without IL3 (Fig. 2A; Supplementary Fig. S4). We determined the cell-based sensitivity of onco-addicted Ba/F3 KANK2-ALK cells to multiple ALK inhibitors, including crizotinib, ceritinib, alectinib, lorlatinib, entrectinib, and brigatinib, using dose–response cell viability assays (Fig. 2B and C; Supplementary Fig. S5). Growth and viability of Ba/F3 KANK2-ALK cell lines were inhibited to varying degrees by all inhibitors tested. Lorlatinib was the most potent inhibitor, exhibiting cell-based 50% inhibitory concentrations ($IC_{50}$) of 0.14 nmol/L. The other inhibitors tested were also effective against KANK2-ALK: crizotinib $IC_{50}$ = 11.3 nmol/L; ceritinib $IC_{50}$ = 10.8 nmol/L; brigatinib $IC_{50}$ = 7.2 nmol/L; entrectinib $IC_{50}$ = 4.2 nmol/L; alectinib $IC_{50}$ = 602 nmol/L. These data demonstrate that multiple ALK inhibitors may be effective against KANK2-ALK fusion–driven cells.

### KANK2-ALK confers anchorage-independent clonal growth of NIH3T3 cells

The propensity of transformed cells to proliferate and survive independent of a solid surface is one of the hallmark properties of neoplastic transformation (43, 44). The soft-agar colony formation assay is an established method for assessing oncogenic activity and malignant transformation using murine NIH3T3 fibroblasts. We engineered a NIH3T3 KANK2-ALK cell line using retrovirus, and performed the soft-agar assay to evaluate colony formation as compared with NIH3T3 parental cells. KANK2-ALK increased the ability of NIH3T3 cells to form colonies in soft agar. Furthermore, colony formation induced by KANK2-ALK was suppressed in a dose-dependent manner with lorlatinib and entrectinib (Fig. 2D and E). On-target inhibition of KANK2-ALK catalytic activity was confirmed biochemically by immunoblotting of lysates generated from stable NIH3T3 KANK2-ALK cell with phospho-ALK antibody (Fig. 2F). Robust inhibition of ALK autophosphorylation is observed with entrectinib and lorlatinib as compared with weaker inhibition with crizotinib.

### KANK2-ALK activity in lineage-specific smooth muscle cells is coupled with RAS/MAPK pathway activation and is ALK inhibitor sensitive

KANK2-ALK functions as a dominant oncogene in both Ba/F3 and NIH3T3 model systems of cell transformation (Fig. 2).

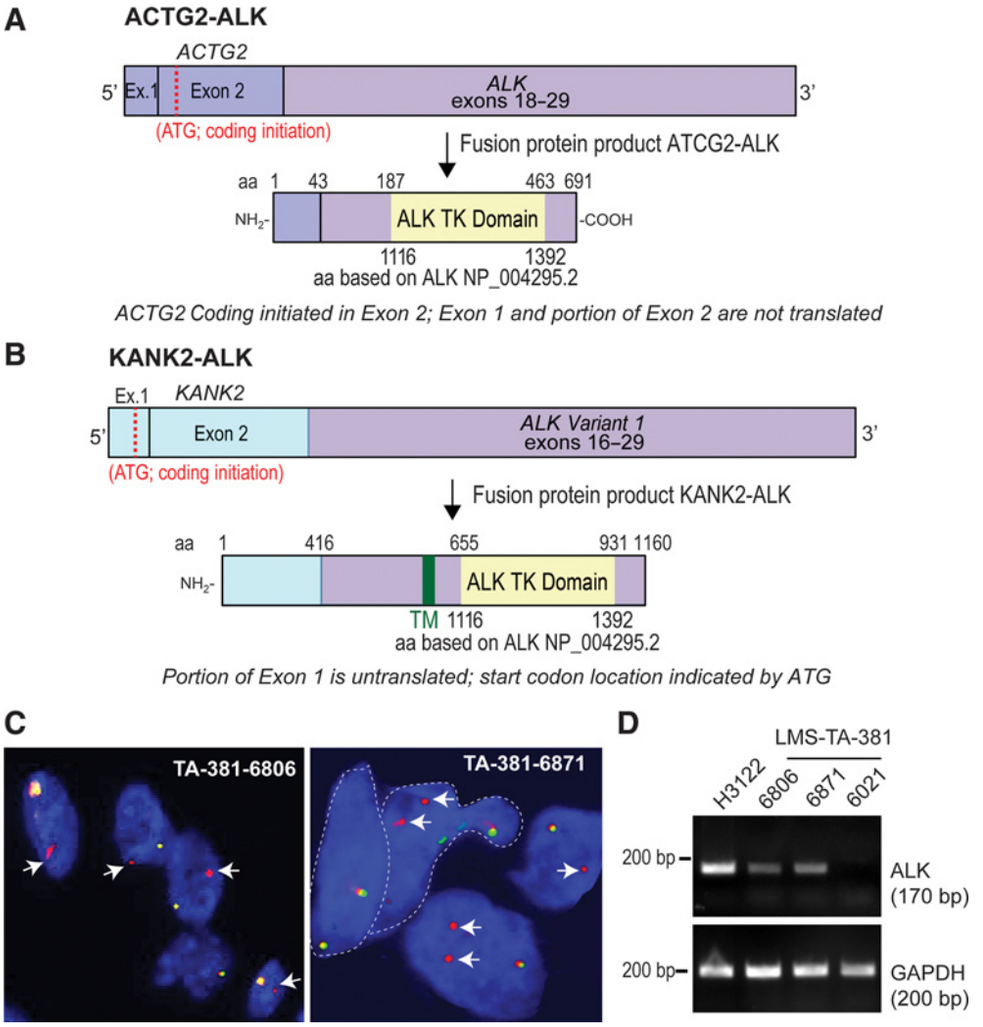


**Figure 1.**

Discovery of ALK fusion genes in leiomyosarcoma. **A** and **B,** Domain organization of the novel ACTG2-ALK and KANK2-ALK fusions (top, mRNA; bottom, protein). TM – indicates the transmembrane domain. **C,** FISH shows chromosomal rearrangement of ALK in two leiomyosarcoma patient samples (TA-381-6806 and TA-381-6871). Both samples were ALK negative by IHC. **D,** RT-PCR using ALK kinase domain–specific primers demonstrates expression of ALK transcript from TA-381-6806 and 6871 leiomyosarcoma samples, but not from a FISH-negative sample, TA-381-6021 (FISH data not shown). cDNA prepared from H3122, an established EML4-ALK positive lung adenocarcinoma cell line, served as a positive control for ALK expression.

Because ALK fusions have not been previously interrogated as drivers of leiomyosarcoma, we wanted to determine whether ectopic expression of an ALK fusion protein is sufficient to induce neoplastic transformation and tumorigenicity in smooth muscle cells, the presumptive cell of origin for leiomyosarcoma (45).

Ba/F3 and NIH3T3 cells are immortalized cell lines, while primary nonneoplastic cells such as mSMCs frequently undergo oncogene-induced senescence in culture. Extensive previous work has demonstrated that deficiency in p53 is critical for neoplastic transformation of primary cells in model systems (44, 46–48). Therefore, we first generated a stable murine smooth muscle cells (mSMC) cell line that expressed a transdominant negative p53 construct (p53DD; refs. 37, 49) followed by serial transduction and selection of KANK2-ALK.

KANK2-ALK is expressed in the transformed mSMCs, and is sensitive to inhibition by lorlatinib, entrectinib, and crizotinib, with lorlatinib being the most potent inhibitor resulting in >50% phospho-inhibition at 10 nmol/L (Fig. 3A). In mSMCs, KANK2-ALK kinase activity is coupled to downstream effector signaling via the canonical RAS/MAPK pathway, as shown by ALK tyrosine kinase inhibitor suppression of ERK phosphorylation in concordance with ALK phospho-inhibition (Fig. 3A). These data suggest that mSMC KANK2-ALK is an adequate lineage-specific model system for determining tumorigenicity *in vivo*.

### KANK2-ALK–driven murine smooth muscle tumors are exquisitely sensitive to lorlatinib *in vivo*

To determine the tumor-forming potential of mSMC KANK2-ALK cells, we performed subcutaneous flank implantation of

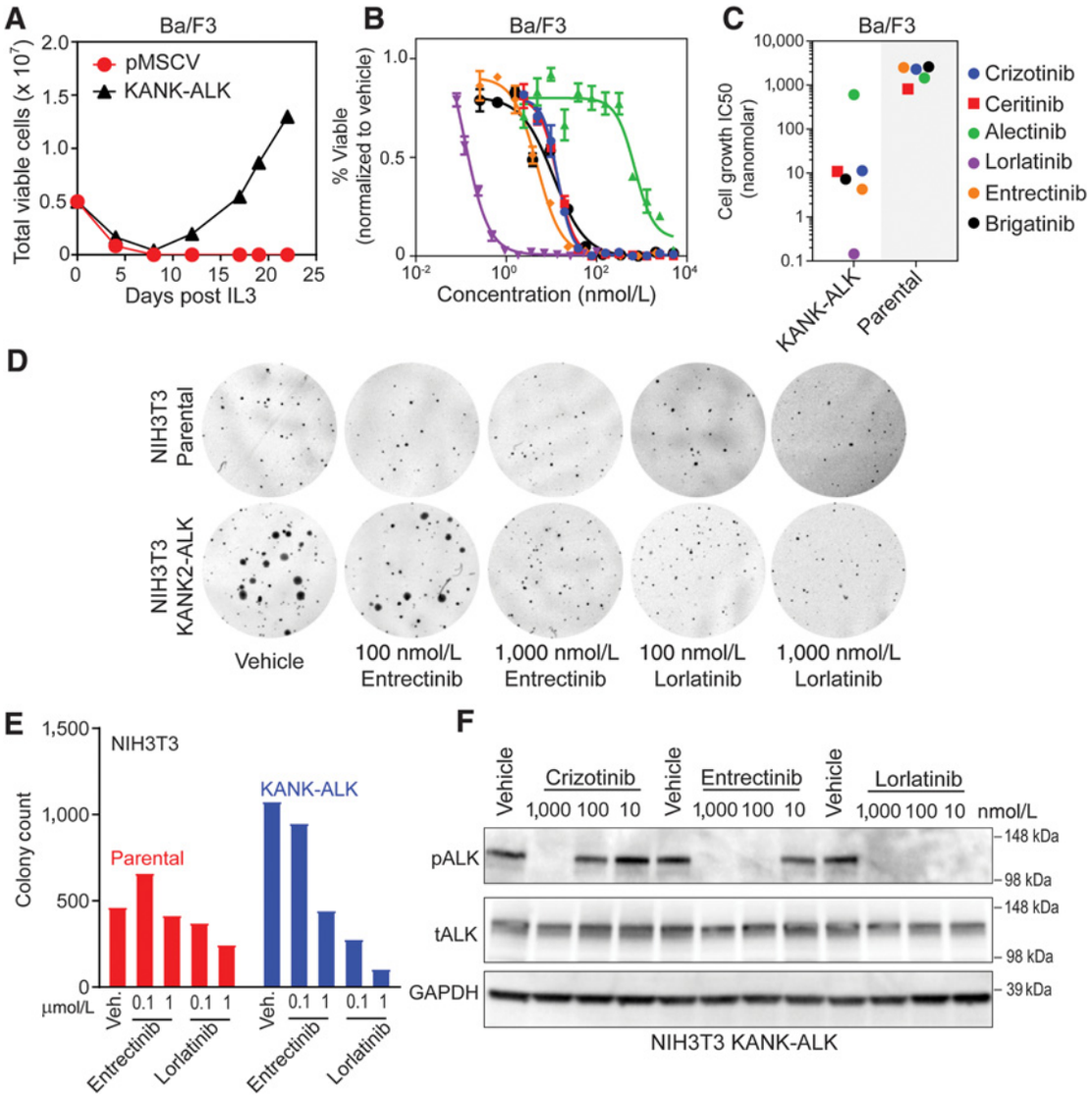


**Figure 2.**

KANK2-ALK is a transforming oncoprotein and sensitive to ALK kinase inhibitors. **A,** Sustained outgrowth of Ba/F3 KANK2-ALK cells, but not pMSCV (empty vector) cells, is observed after IL3 withdrawal. **B,** Dose–response assay of Ba/F3 KANK2-ALK cells after 72-hour exposure to multiple ALK inhibitors. Data are normalized to vehicle-treated control, and values shown are the mean ± SEM. **C,** Scatter plot of cell proliferation $IC_{50}$ values for each ALK inhibitor against Ba/F3 KANK2-ALK cells. Colored symbols represent different inhibitors as shown on the right. **D,** Anchorage-independent colony-forming assay using stable NIH3T3 KANK2-ALK cells demonstrates colony formation with dose-dependent inhibition by entrectinib and lorlatinib. **E,** Quantification of colony formation by NIH3T3 parental and KANK2-ALK cells with dose-dependent inhibition by entrectinib and lorlatinib. **F,** Immunoblot analysis of phospho-ALK (pALK), total ALK (tALK), and GAPDH (loading control) of lysates prepared from NIH3T3 KANK2-ALK cells after 4-hour treatment with three different ALK inhibitors at indicated concentrations. Representative immunoblot images from one of three independent experiments are shown.

these engineered mSMCs in Nu/Nu mice. For longitudinal monitoring of cell engraftment and tumor growth using noninvasive bioluminescent imaging, the mSMC p53DD (control) and mSMC p53DD, KANK2-ALK cells were lentivirally engineered and selected to stably express *Renilla* luciferase. Luciferase-positive tumor cell engraftment and nascent tumor formation is apparent on day 3 after injection of KANK2-ALK cells but not of mSMC p53DD cells (Fig. 3B). Tumor volume was measurable using calipers by day 14. Nineteen days after implantation, the mSMC KANK2-ALK tumors reached a volume of 0.2 $cm^3$. At this time, the mice were randomized into three cohorts and treated with vehicle, crizotinib, or lorlatinib by oral gavage. Lorlatinib resulted in near immediate tumor regression (Fig. 3C). Treatment continued for 4 weeks or until tumor volume exceeded 2 $cm^3$, at which point animals were humanely sacrificed. Median survival of tumor-bearing mice improved modestly with crizotinib treatment (36 vs. 47 days), but was significantly extended with lorlatinib treatment (median OS not achieved, $P < 0.001$; Fig. 3D). Mice in the

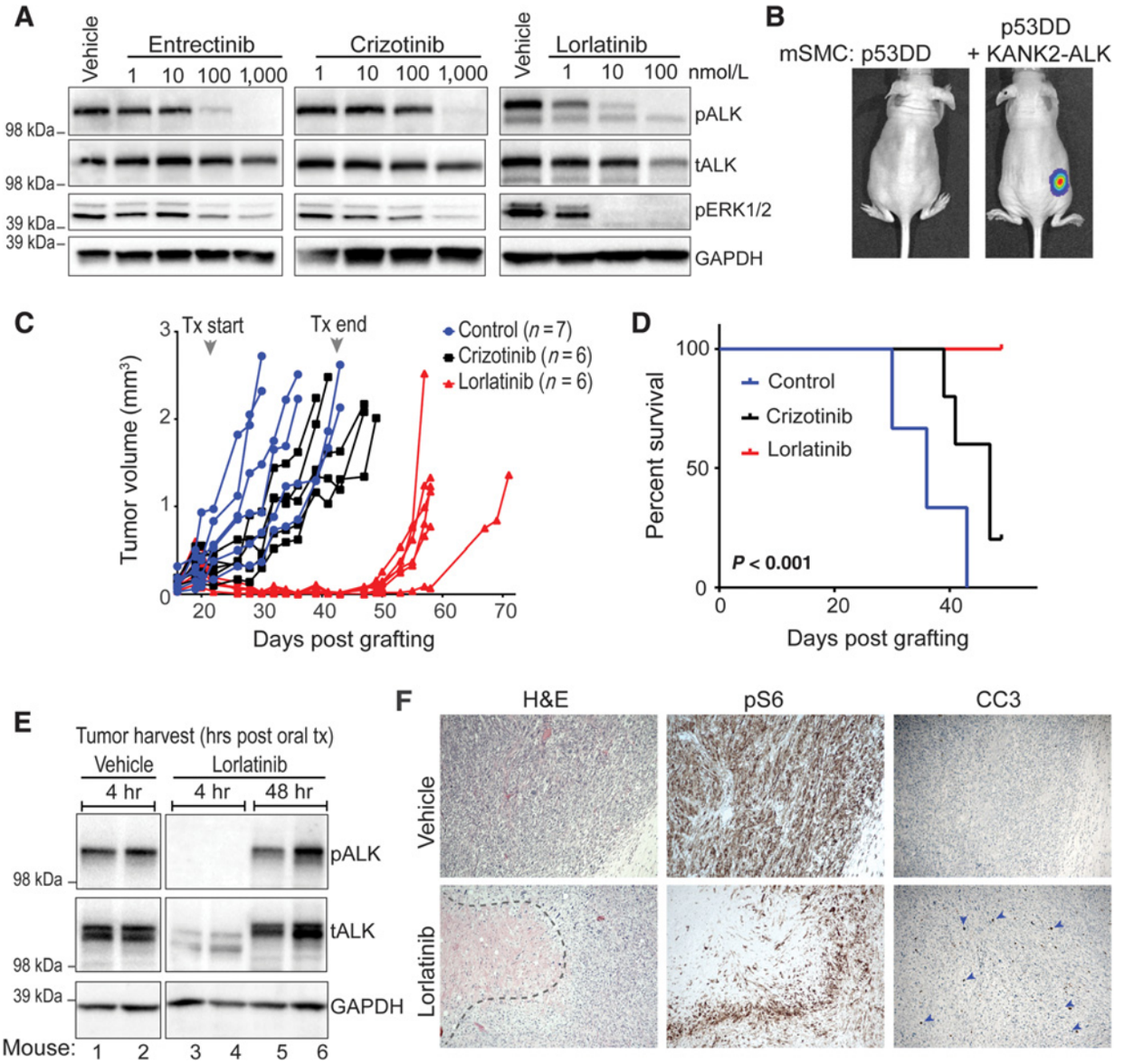


**Figure 3.**

KANK2-ALK–driven smooth muscle cell tumors are highly sensitive to lorlatinib *in vivo*. **A,** Immunoblot analysis of phospho-ALK (pALK), total ALK (tALK), phospho-ERK (pERK1/2), and GAPDH (loading control) of lysates prepared from murine smooth muscle KANK2-ALK cells (mSMC) after 4-hour treatment with three different ALK inhibitors at indicated concentrations. **B,** IVIS bioluminescence imaging of mSMC p53DD compared with mSMC p53DD + KANK2-ALK; imaging performed 3 days after flank cell injection. **C,** Tumor volume of mice harboring mSMC p53DD + KANK2-ALK as measured by calipers. Treatment (Tx) began when tumor volume reached 0.2 $mm^3$ [Tx arrowhead (gray)] and continued for 4 weeks. **D,** Kaplan–Meier survival analysis of treated animals. **E,** Immunoblot analysis of phospho-ALK (pALK), total ALK (tALK), and GAPDH (loading control) of lysates prepared from vehicle-treated compared with lorlatinib-treated mice. Lanes 3 and 4 contain lysate from tumors harvested 4 hours after the last dose of lorlatinib. Lanes 5 and 6 contain lysate from tumors harvested 48 hours after last dose of lorlatinib. **F,** Hematoxylin and eosin (H&E) stain and IHC from mSMC p53DD + KANK2-ALK tumors treated with vehicle (top row) or lorlatinib (bottom row). IHC was performed with phospho-S6 (pS6), and cleaved caspase-3 (CC3)-directed antibodies.

lorlatinib cohort were followed over time and developed measurable tumors 10–15 days after drug discontinuation (Fig. 3C).

To assess on-target inhibition of KANK2-ALK catalytic activity, mice were orally treated with lorlatinib for five days and tissue was harvested following last treatment for immunoblotting with phospho- and total ALK antibodies (Fig. 3E). Lorlatinib treatment abrogated phospho-ALK as hypothesized. Loss of phospho-ALK is concomitant with decrease of total ALK level in lorlatinib versus untreated tumors that is presumably via protein destabilization and degradation as has been previously reported for EML4-ALK variants (50). Both phospho- and total ALK levels are restored to control levels at 48 hours after

lorlatinib treatment was stopped (Fig. 3E, lanes 5 and 6). IHC of lorlatinib-treated tumors confirms downstream ALK effector signaling as evidenced by diminished phospho-S6 staining concurrent with areas of necrosis, and induction of apoptosis as seen by hematoxylin and eosin (H&E) and cleaved caspase-3 staining (Fig. 3F).

## Discussion

Over the last decade, implementation of advanced next-generation sequencing (NGS) technologies in molecular pathology and clinical diagnostics has enabled the discovery of novel oncogenic drivers, permitted tumor reclassification and, in some cases, guided treatment decisions. Targeted therapy directed at a dominant oncogenic driver has dramatically altered survival outcomes in subsets of patients from diverse malignancies including chronic myeloid leukemia, NSCLC, and GIST (26, 51, 52). However, not all patients with cancer have benefitted from these advancements yet, particularly patients with rare cancer subtypes.

Soft-tissue sarcomas are uncommon cancers with a high degree of histologic and genomic heterogeneity, which has stymied the development of effective new treatment strategies. The recent characterization of these tumors by TCGA offers new opportunities for unraveling disease biology and uncovering pharmacologically targetable vulnerabilities (13). By interrogating these data as well as similar NGS data from Foundation Medicine (14, 15), we have found that a subset of leiomyosarcoma tumors harbor ALK fusions that retain the ALK kinase domain.

The KANK2-ALK and ACTG2-ALK fusions reported here contain 5′ fusion partner genes that have not previously been validated in cancer. Notably, these ALK fusions have breakpoints within introns 15 (KANK2-ALK) or 17 (ACTG2-ALK), as opposed to the previously reported and more common intron 19 breakpoint fusions such as in case of EML4-ALK (38). We have shown that KANK2-ALK has robust oncogenic potential and is sensitive to ALK inhibitors—similar to ALK fusions with intron 19 breakpoint.

Because ACTG2 and ALK are located in opposite orientations on chromosome 2p, the formation of ACTG2-ALK is likely a cryptic paracentric inversion mechanism, which is distinct from EML4-ALK formation and not detectable by karyotyping or comparative genomic hybridization (CGH). FISH results may also be misleading in some cases. In our study, the FISH-positive leiomyosarcoma cells (Fig. 1C) demonstrate loss of the 5′ region of ALK. While this may represent a false-positive, this pattern is consistent with the presence of an unbalanced translocation, a common mechanism in lymphomas and IMTs (53). Alternatively, loss of the 5′ signal is also seen in fusions generated from intrachromosomal deletion, such as those known to occur in the ALK paralog, ROS1 (54). Future studies in which sufficient material is available could compare results of FISH with sequencing data to better establish the rate of FISH false-positive results.

The difficulty in fusion gene discovery extends beyond paracentric inversions, unbalanced translocations, and intrachromosomal deletions. Even with NGS data, the bioinformatic analytic processes routinely applied for mutation or copy number analyses are often inadequate. The ongoing development of advanced algorithms for fusion detection [e.g., STAR-Fusion (32), ChimeraScan (33), deFuse (34), FusionCatcher (35)] is resulting in higher sensitivity and specificity in detecting and calling fusion genes.

In cancer cells, various structural rearrangements may exist at the genomic level, but whether the chimeric fusion protein is expressed or not is largely dictated by the transcriptional activity at the promoter of the 5′ fusion partner gene. Thus, we can posit that the expression of the 5′ partner gene is a form of selection pressure dictating which chromosomal translocations are present in diverse cancer cell lineages. Given this hypothesis, it is interesting to note that *ACTG2* codes for enteric smooth muscle actin gamma 2, a protein that is highly expressed in smooth muscle cells within the gastrointestinal and genitourinary system (55). Therefore, it is rational that the *ACTG2* promoter drives expression of an oncogenic ACTG2-ALK fusion gene in a smooth muscle cell, ultimately resulting in a leiomyosarcoma. In fact, ACTG2 has been used as an IHC marker to identify subtype 1 leiomyosarcomas, which have a gene expression profile more similar to normal smooth muscle than other leiomyosarcoma subtypes (36). Similarly, *KANK2* encodes an ankyrin domain–containing cytoskeletal regulatory protein that is robustly expressed in smooth muscle and uterus, again suggestive of selection of these fusions in smooth muscle tumors due to active promoters driving expression of the ALK fusion (55).

Having received FDA approval in 2011, crizotinib is a well-established the first-generation ALK inhibitor in clinical use. However, the pharmacologic pipeline for targeting ALK is expanding, with four drugs now FDA-approved and several other agents in various stages of development (24–30). Lorlatinib is currently in phase III clinical trials, most notably being evaluated against crizotinib for first-line treatment of patients with ALK-positive NSCLC (NCT03052608). Given the exquisite sub- to low nanomolar *in vitro* sensitivity of Ba/F3 ACTG2-ALK and KANK2-ALK cells to lorlatinib, we compared efficacy of oral monotherapy with crizotinib and lorlatinib in the murine model of KANK2-ALK leiomyosarcoma. Crizotinib offered only modest benefit both in terms of survival and inhibition of tumor growth, while lorlatinib induced statistically significant tumor regression and prolonged survival. This effect is despite the use of relatively high doses of crizotinib (100 mg/kg daily) and moderate doses of lorlatinib (3 mg/kg). Notably, *in vitro* treatment of NIH3T3 and mSMC KANK2-ALK cells with crizotinib showed similar weak inhibitory activity. A similar trend was previously observed in a ROS1 fusion–driven murine cholangiocarcinoma model, where *in vivo* efficacy of oral crizotinib was modest as compared with type II ROS1 inhibitor, foretinib (56). Lorlatinib was specifically engineered to exhibit high potency and is effective against multiple cancer types *in vitro* and *in vivo* at lower doses than crizotinib (57–59). In addition, we postulate that structural differences in the KANK2-ALK fusion protein may lead to improved binding of lorlatinib as compared with crizotinib, as it retains Exon 16 and therefore a considerable amount of the juxtamembrane region preceding the kinase domain, which may influence binding pocket conformation. Future studies using molecular dynamic simulation may explain the observed differences in inhibitor efficacy.

The presence of an ALK rearrangement in a soft-tissue tumor is most often associated with inflammatory myofibroblastic tumor (IMT). Although both IMT and leiomyosarcoma are mesenchymal soft-tissue neoplasms, each have with distinct histology, epidemiology and metastatic potential. In contrast to leiomyosarcoma, IMT occurs primarily in children and young adults and rarely metastasizes. IMT is a distinctive tumor with an abundance of inflammatory infiltrate and fibroblastic

spindle cells and is easily distinguishable from leiomyosarcoma by an experienced sarcoma pathologist. Up to 70% of IMTs contain clonal rearrangements involving ALK (12). The tumors harboring ACTG2-ALK and KANK2-ALK included in our analyses were TCGA specimens; as such, these samples were evaluated by multiple sarcoma pathologists and confirmed to be leiomyosarcoma. Thus, the presence of an ALK rearrangement does not change the histologic diagnosis arrived at by morphologic and IHC assessment. In addition, these ALK fusions have not been previously reported in IMT.

The Cancer Genome Atlas sarcoma dataset includes next-generation sequencing of DNA and RNA as well as additional in-depth molecular evaluations that would not typically be obtained as part of clinical care. Even with the depth of these raw data and detailed, expert analyses, ACTG2-ALK and KANK2-ALK fusions were not previously identified. However, systematic, hypothesis-based interrogation of existing datasets, such as the approach employed here, may yield clinically meaningful discoveries of targetable oncogenes in sarcoma.

With improving ability to detect rearrangements and multiple highly effective and safe treatment options for ALK-positive disease, we believe advanced molecular diagnostics should be employed more often in the sarcoma patient population. Cumulatively, our data suggest that ALK and potentially other targetable kinase fusions may be present in subsets of soft-tissue sarcoma patients, and their discovery may propel new therapeutic strategies in this treatment-refractory cancer.

## Disclosure of Potential Conflicts of Interest

No potential conflicts of interest were disclosed.

## Authors' Contributions

**Conception and design:** L.E. Davis, K. Nusser, M.A. Davare
**Development of methodology:** L.E. Davis, K. Nusser, J. Przybyl, N.E. Hofmann, M. Debiec-Rychter, M.A. Davare
**Acquisition of data (provided animals, acquired and managed patients, provided facilities, etc.):** L.E. Davis, K. Nusser, J. Przybyl, N.E. Hofmann, M. van de Rijn, M.A. Davare
**Analysis and interpretation of data (e.g., statistical analysis, biostatistics, computational analysis):** L.E. Davis, K. Nusser, J. Przybyl, S. Varma, S. Vennam, M. Debiec-Rychter, M. van de Rijn, M.A. Davare
**Writing, review, and/or revision of the manuscript:** L.E. Davis, K. Nusser, J. Przybyl, M. Debiec-Rychter, M. van de Rijn, M.A. Davare
**Administrative, technical, or material support (i.e., reporting or organizing data, constructing databases):** L.E. Davis, K. Nusser, J. Pittsenbarger, N.E. Hofmann, M.A. Davare
**Study supervision:** L.E. Davis, M.A. Davare

## Acknowledgments

This work was supported by the Knight Cancer Institute Pilot Grant (intramural).

The costs of publication of this article were defrayed in part by the payment of page charges. This article must therefore be hereby marked *advertisement* in accordance with 18 U.S.C. Section 1734 solely to indicate this fact.

Received October 4, 2018; revised October 28, 2018; accepted November 27, 2018; published first December 5, 2018.

## References

1. Weitz J, Antonescu CR, Brennan MF. Localized extremity soft tissue sarcoma: improved knowledge with unchanged survival over time. J Clin Oncol 2003;21:2719–25.
2. Judson I, Verweij J, Gelderblom H, Hartmann JT, Schöffski P, Blay JY, et al. Doxorubicin alone versus intensified doxorubicin plus ifosfamide for first-line treatment of advanced or metastatic soft-tissue sarcoma: a randomised controlled phase 3 trial. Lancet Oncol 2014;15:415–23.
3. Iasonos A, Keung EZ, Zivanovic O, Mancari R, Peiretti M, Nucci M, et al. External validation of a prognostic nomogram for overall survival in women with uterine leiomyosarcoma. Cancer 2013;119:1816–22.
4. Davare MA, Tognon CE. Detecting and targetting oncogenic fusion proteins in the genomic era. Biol Cell 2015;107:111–29.
5. Rutkowski P, Van Glabbeke M, Rankin CJ, Ruka W, Rubin BP, Debiec-Rychter M, et al. Imatinib mesylate in advanced dermatofibrosarcoma protuberans: pooled analysis of two phase II clinical trials. J Clin Oncol 2010;28:1772–9.
6. Doebele RC, Davis LE, Vaishnavi A, Le AT, Estrada-Bernal A, Keysar S, et al. An oncogenic NTRK fusion in a patient with soft-tissue sarcoma with response to the tropomyosin-related kinase inhibitor LOXO-101. Cancer Discov 2015;5:1049–57.
7. Cassier PA, Gelderblom H, Stacchiotti S, Thomas D, Maki RG, Kroep JR, et al. Efficacy of imatinib mesylate for the treatment of locally advanced and/or metastatic tenosynovial giant cell tumor/pigmented villonodular synovitis. Cancer 2012;118:1649–55.
8. Joensuu H, Eriksson M, Sundby Hall K, et al. One vs three years of adjuvant imatinib for operable gastrointestinal stromal tumor: a randomized trial. JAMA 2012;307:1265–72.
9. American Cancer Society. American Cancer Society Cancer Facts and Figures 2017. Atlanta, GA: American Cancer Society; 2017.
10. Serrano C, George S. Leiomyosarcoma. Hematol Oncol Clin North Am 2013;27:957–74.
11. Toro JR, Travis LB, Wu HJ, Zhu K, Fletcher CD, Devesa SS. Incidence patterns of soft tissue sarcomas, regardless of primary site, in the surveillance, epidemiology and end results program, 1978–2001: an analysis of 26,758 cases. Int J Cancer 2006;119:2922–30.
12. Fletcher CDM, World Health Organization, International Agency for Research on Cancer. WHO classification of tumours of soft tissue and bone. Lyon, France: IARC Press; 2013.
13. The Cancer Genome Atlas Research Network. Comprehensive and integrated genomic characterization of adult soft tissue sarcomas. Cell 2017;171:950–65.
14. Morosini D, Chmielecki J, Goldberg M, Ross J, Stephens P, Miller V, et al. Comprehensive genomic profiling of sarcomas from 267 adolescents and young adults to reveal a spectrum of targetable genomic alterations. J Clin Oncol 33:15s, 2015 (suppl; abstr 11020).
15. Elvin JA, Chalmers ZR, Chiemlicki J, Wang KAI, Palma N, Ali SM, et al. Genomic profiling of uterine leiomyosarcomas reveal frequent alterations in Akt/mammalian target of rapamycin (mTOR) pathway genes and other actionable genomic abnormalities linked to targeted therapies. Eur J Cancer 2014:50 (Suppl 6):104.
16. Pulford K, Morris SW, Turturro F. Anaplastic lymphoma kinase proteins in growth control and cancer. J Cell Physiol 2004;199:330–58.
17. Katayama R, Lovly CM, Shaw AT. Therapeutic targeting of anaplastic lymphoma kinase in lung cancer: a paradigm for precision cancer medicine. Clin Cancer Res 2015;21:2227–35.
18. Alexander RE, Montironi R, Lopez-Beltran A, Williamson SR, Wang M, Post KM, et al. EGFR alterations and EML4-ALK rearrangement in primary adenocarcinoma of the urinary bladder. Mod Pathol 2014;27:107–12.
19. Lee J, Kim HC, Hong JY, Wang K, Kim SY, Jang J, et al. Detection of novel and potentially actionable anaplastic lymphoma kinase (ALK) rearrangement in colorectal adenocarcinoma by immunohistochemistry screening. Oncotarget 2015;6:24320–32.
20. Perot G, Soubeyran I, Ribeiro A, Bonhomme B, Savagner F, Boutet-Bouzamondo N, et al. Identification of a recurrent STRN/ALK fusion in thyroid carcinomas. PLoS One 2014;9:e87170.
21. Xing X, Lin D, Ran W, Liu H. ALK-positive diffuse large B-cell lymphoma of the duodenum: a case report and review of the literature. Exp Ther Med 2014;8:409–12.

22. Lovly CM, Gupta A, Lipson D, Otto G, Brennan T, Chung CT, et al. Inflammatory myofibroblastic tumors harbor multiple potentially actionable kinase fusions. Cancer Discov 2014;4:889–95.
23. Haimes JD, Stewart CJR, Kudlow BA, Culver BP, Meng B, Koay E, et al. Uterine inflammatory myofibroblastic tumors frequently harbor ALK fusions with IGFBP5 and THBS1. Am J Surg Pathol 2017;41:773–80.
24. Awad MM, Shaw AT. ALK inhibitors in non-small cell lung cancer: crizotinib and beyond. Clin Adv Hematol Oncol 2014;12:429–39.
25. Casaluce F, Sgambato A, Maione P, Rossi A, Ferrara C, Napolitano A, et al. ALK inhibitors: a new targeted therapy in the treatment of advanced NSCLC. Target Oncol 2013;8:55–67.
26. Shaw AT, Kim DW, Nakagawa K, Seto T, Crino L, Ahn MJ, et al. Crizotinib versus chemotherapy in advanced ALK-positive lung cancer. N Engl J Med 2013;368:2385–94.
27. Shaw AT, Kim DW, Mehra R, Tan DS, Felip E, Chow LQ, et al. Ceritinib in ALK-rearranged non-small-cell lung cancer. N Engl J Med 2014; 370:1189–97.
28. Soda M, Choi YL, Enomoto M, Takada S, Yamashita Y, Ishikawa S, et al. Identification of the transforming EML4-ALK fusion gene in non-small-cell lung cancer. Nature 2007;448:561–6.
29. Drilon A, Siena S, Ou SI, Patel M, Ahn MJ, Lee J, et al. Safety and antitumor activity of the multitargeted Pan-TRK, ROS1, and ALK inhibitor entrectinib: combined results from two phase I trials (ALKA-372–001 and STARTRK-1). Cancer Discov 2017;7:400–9.
30. Shaw AT, Felip E, Bauer TM, Besse B, Navarro A, Postel-Vinay S, et al. Lorlatinib in non-small-cell lung cancer with ALK or ROS1 rearrangement: an international, multicentre, open-label, single-arm first-in-man phase 1 trial. Lancet Oncol 2017;18:1590–9.
31. Tryka KA, Hao L, Sturcke A, Jin Y, Wang ZY, Ziyabari L, et al. NCBI's Database of genotypes and phenotypes: dbGaP. Nucleic Acids Res 2014; 42:D975–9.
32. Haas B, Dobin A, Stransky N, Li B, Yang X, Tickle T, et al. STAR-Fusion: fast and accurate fusion transcript detection from RNA-Seq. bioRxiv 2017. Available from: https://doi.org/10.1101/120295.
33. Iyer MK, Chinnaiyan AM, Maher CA. ChimeraScan: a tool for identifying chimeric transcription in sequencing data. Bioinformatics 2011;27:2903–4.
34. McPherson A, Hormozdiari F, Zayed A, Giuliany R, Ha G, Sun MG, et al. deFuse: an algorithm for gene fusion discovery in tumor RNA-Seq data. PLoS Comput Biol 2011;7:e1001138.
35. Nicorici D, Satalan M, Edgren H, Kangaspeska S, Murumagi A, Kallioniemi O, et al. FusionCatcher - a tool for finding somatic fusion genes in paired-end RNA-sequencing data. bioRxiv 2014. Available from: https://doi.org/10.1101/011650.
36. Guo X, Jo VY, Mills AM, Zhu SX, Lee CH, Espinosa I, et al. Clinically relevant molecular subtypes in leiomyosarcoma. Clin Cancer Res 2015;21:3501–11.
37. Hong H, Takahashi K, Ichisaka T, Aoi T, Kanagawa O, Nakagawa M, et al. Suppression of induced pluripotent stem cell generation by the p53-p21 pathway. Nature 2009;460:1132–5.
38. Shaw AT, Hsu PP, Awad MM, Engelman JA. Tyrosine kinase gene rearrangements in epithelial malignancies. Nat Rev Cancer 2013;13:772–87.
39. Shah N, Lankerovich M, Lee H, Yoon JG, Schroeder B, Foltz G. Exploration of the gene fusion landscape of glioblastoma using transcriptome sequencing and copy number data. BMC Genomics 2013;14:818.
40. Cerami E, Gao J, Dogrusoz U, Gross BE, Sumer SO, Aksoy BA, et al. The cBio cancer genomics portal: an open platform for exploring multidimensional cancer genomics data. Cancer Discov 2012;2:401–4.
41. Thorvaldsdottir H, Robinson JT, Mesirov JP. Integrative genomics viewer (IGV): high-performance genomics data visualization and exploration. Brief Bioinform 2013;14:178–92.
42. Warmuth M, Kim S, Gu XJ, Xia G, Adrian F. Ba/F3 cells and their use in kinase drug discovery. Curr Opin Oncol 2007;19:55–60.
43. Borowicz S, Van Scoyk M, Avasarala S, Karuppusamy Rathinam MK, Tauler J, Bikkavilli RK, et al. The soft agar colony formation assay. J Vis Exp 2014: e51998.
44. Hanahan D, Weinberg RA. Hallmarks of cancer: the next generation. Cell 2011;144:646–74.
45. Miettinen M. Smooth muscle tumors of soft tissue and non-uterine viscera: biology and prognosis. Mod Pathol 2014;27:S17–29.
46. Courtois-Cox S, Jones SL, Cichowski K. Many roads lead to oncogene-induced senescence. Oncogene 2008;27:2801–9.
47. Serrano M, Lin AW, McCurrach ME, Beach D, Lowe SW. Oncogenic ras provokes premature cell senescence associated with accumulation of p53 and p16INK4a. Cell 1997;88:593–602.
48. Lowe S, Cifra A. Exploring cell apoptosis and senescence to understand and treat cancer: an interview with Scott Lowe. Dis Model Mech 2015; 8:1345–8.
49. Bowman T, Symonds H, Gu L, Yin C, Oren M, Van Dyke T. Tissue-specific inactivation of p53 tumor suppression in the mouse. Genes Dev 1996; 10:826–35.
50. Heuckmann JM, Balke-Want H, Malchers F, Peifer M, Sos ML, Koker M, et al. Differential protein stability and ALK inhibitor sensitivity of EML4-ALK fusion variants. Clin Cancer Res 2012;18:4682–90.
51. Druker BJ, Guilhot F, O'Brien SG, Gathmann I, Kantarjian H, Gattermann N, et al. Five-year follow-up of patients receiving imatinib for chronic myeloid leukemia. N Engl J Med 2006;355:2408–17.
52. Demetri GD, von Mehren M, Blanke CD, Van den Abbeele AD, Eisenberg B, Roberts PJ, et al. Efficacy and safety of imatinib mesylate in advanced gastrointestinal stromal tumors. N Engl J Med 2002;347:472–80.
53. van der Krogt JA, Bempt MV, Ferreiro JF, Mentens N, Jacobs K, Pluys U, et al. Anaplastic lymphoma kinase-positive anaplastic large cell lymphoma with the variant RNF213-, ATIC- and TPM3-ALK fusions is characterized by copy number gain of the rearranged ALK gene. Haematologica 2017; 102:1605–16.
54. Davare MA, Henderson JJ, Agarwal A, Wagner JP, Iyer SR, Shah N, et al. Rare but recurrent ROS1 fusions resulting from chromosome 6q22 microdeletions are targetable oncogenes in glioma. Clin Cancer Res 2018;24:6471–82.
55. Fagerberg L, Hallstrom BM, Oksvold P, Kampf C, Djureinovic D, Odeberg J, et al. Analysis of the human tissue-specific expression by genome-wide integration of transcriptomics and antibody-based proteomics. Mol Cell Proteomics 2014;13:397–406.
56. Davare MA, Saborowski A, Eide CA, Tognon C, Smith RL, Elferich J, et al. Foretinib is a potent inhibitor of oncogenic ROS1 fusion proteins. Proc Natl Acad Sci USA 2013;110:19519–24.
57. Zou Helen Y, Friboulet L, Kodack David P, Engstrom Lars D, Li Q, West M, et al. PF-06463922, an ALK/ROS1 inhibitor, overcomes resistance to first and second generation ALK inhibitors in preclinical models. Cancer Cell 2015;28:70–81.
58. Johnson TW, Richardson PF, Bailey S, Brooun A, Burke BJ, Collins MR, et al. Discovery of (10R)-7-Amino-12-fluoro-2,10,16-trimethyl-15-oxo-10,15,16,17-tetrahydro-2H-8,4-(metheno)pyrazolo[4,3-h][2,5,11]-benzoxadiazacyclotetradecine-3-carbonitrile (PF-06463922), a macrocyclic inhibitor of anaplastic lymphoma kinase (ALK) and c-ros oncogene 1 (ROS1) with preclinical brain exposure and broad-spectrum potency against ALK-resistant mutations. J Med Chem 2014;57:4720–44.
59. Infarinato NR, Park JH, Krytska K, Ryles HT, Sano R, Szigety KM, et al. The ALK/ROS1 inhibitor PF-06463922 overcomes primary resistance to crizotinib in ALK-driven neuroblastoma. Cancer Discov 2016;6:96–107.